**NASA Technical Paper 2032**

July 1982

# Buckling Test of a 3-Meter-Diameter Corrugated Graphite-Epoxy Ring-Stiffened Cylinder

Randall C. Davis



NASA

NASA
Technical
Paper
2032

1982

# Buckling Test of a 3-Meter-Diameter Corrugated Graphite-Epoxy Ring-Stiffened Cylinder

Randall C. Davis
*Langley Research Center*
*Hampton, Virginia*

National Aeronautics
and Space Administration

**Scientific and Technical
Information Branch**

## SUMMARY

A 3-m-diameter by 3-m-long corrugated cylindrical shell with external stiffening rings was tested to failure by buckling. The corrugation geometry for the graphite-epoxy composite cylinder wall was optimized to withstand a compressive load producing the relatively low maximum load intensity of 157.6 kN/m without buckling. The resulting mass per unit of shell-wall area, including stiffening rings and fasteners, was 1.96 $kg/m^2$. The cylinder test-load achievement of 101 percent of design ultimate demonstrates a substantial mass-saving potential over available data for corrugated aluminum shell designs.

## INTRODUCTION

Future space missions, such as those involving a space tug or shuttle, will require low-mass structures to achieve maximum payloads. For such structures that must carry compression loads without buckling, graphite-epoxy materials offer an attractive approach to providing the needed low-mass structural components. Preliminary design studies of lightly loaded shells, using minimum-mass structural-sizing codes, indicate that ring-stiffened graphite-epoxy corrugated shells can, like corrugated graphite-epoxy panels (refs. 1 and 2), offer a mass-saving potential of 20 to 40 percent over aluminum shell-wall design concepts. To evaluate the merits of a corrugated graphite-epoxy cylindrical shell and to develop a design data base for lightweight space structures, a program was initiated to design, fabricate, and test a 3-m-diameter by 3-m-long corrugated ring-stiffened graphite-epoxy cylinder.

The preliminary design for the cylinder was generated using a minimum-mass structural-sizing code (ref. 3) to carry an ultimate axial-compression loading intensity of 157.6 kN/m. The preliminary design for the shell was modified and verified by testing subcomponent specimens as described in reference 4. The shell wall was fabricated from three flat corrugated sheets wrapped to the proper cylindrical shape as described in references 5 through 7. The test method used to produce the load intensity was to mount the specimen as a cantilevered cylinder and apply a pure bending moment to the end. Studies by Seide (ref. 8) have shown that for length-to-diameter ratios of the order of 1.0, the same buckling behavior occurs on the compression side of the cylinder in bending as for axial compression. The purpose of this paper is to present the results from the test of the cylinder.

## TEST SPECIMEN

The overall configuration of the 3-m-diameter shell (described in detail in refs. 4 through 7) consists of a corrugated wall stiffened with four external stiffener rings spaced at 60.96-cm intervals along the 3.05-m length of the shell, as shown in figure 1. The total length of the specimen is 3.15 m including the steel loading rings which serve as connecting interfaces with the test machine that applies the bending moment to the shell. The open corrugations, running the length of the cylinder, have a pitch of 11.40 cm in the circumferential direction and a crown, or flat, width of 3.650 cm.

The graphite-epoxy material (table 1) used for fabricating the cylinder wall and stiffener rings in this investigation was Union Carbide Thornel 300 graphite fibers preinpregnated with Normco 5208 epoxy resin, the material being obtained in 30.48-cm-wide tape form. The layup for the corrugated wall consists of four plies of symmetric ±45° fibers with five plies of 0° reinforcing longitudinals sandwiched between the ±45° plies at each crown. (See fig. 1.) To substantiate the computed stiffness properties for the shell-wall material, tensile test coupons were cut from an undamaged section of the cylinder wall after the test. Six coupons each were made from the crowns and from the webs of the wall section. Each coupon was instrumented with electrical resistance strain gages to measure longitudinal and transverse strains. Stiffness values and transverse contractions from the load-strain data for these coupon tests were averaged for the tabulation shown in table 2. As the tabulated results show, there is good agreement between the experimental values and the analytical values computed using the nominal lamina properties shown in table 1. The average ply thickness from the measurements was 0.0132 cm for the crown coupons and 0.0130 cm for the web coupons.

The stiffener rings have a closed-hat cross section consisting of four symmetric plies of ±45° fibers, and the base strip for the closed-hat section has a $[\pm 45/0_2/\pm 45]$ layup. The stiffener rings were adhesively bonded and riveted to the crowns of the cylinder wall. Scalloped attachment rings, made of aluminum, were mechanically attached to each end of the cylinder to transfer the applied load to the corrugated shell wall. The corrugation crowns underneath the scalloped attachment rings were locally reinforced with additional 0° doubler plies that tapered in steps down to the basic shell-wall geometry as shown in figure 1 and described in detail in references 4 through 7.

## APPARATUS AND CYLINDER TEST PROCEDURE

The applied bending load is introduced into the shell wall by the set of concentric scalloped attachment rings bolted to each end of the cylinder. These scalloped attachment rings are bolted to angle-section aluminum adapter rings to transfer the applied load from the loading rings to the scalloped attachment rings. (See figs. 1 through 3.) The loading rings are bolted to conical loading fixtures as shown in figure 4. The conical loading fixture at one end of the cylinder is mounted to a rigid wall. The conical loading fixture at the other end of the cylinder is attached to a triangular loading frame that applies the bending load through two loading arms. (See fig. 4.) These arms apply equal and opposite loads to the conical loading fixtures through an end-plate fixture. The loading arms pivot about pins in the triangular loading frame and in the end plate to allow the test cylinder freedom to rotate and to move upward under the action of the applied bending load. The masses of the conical fixture, loading ring, and end plate are balanced by two counterweights connected to two balance beams mounted on top of a pair of end-fixture support beams above the cylinder.

The triangular loading frame rotates about a main pivot pin through its vertical leg and the two floor supports bolted to the laboratory floor. (See fig. 4.) Loaded as described, the cylinder receives axial-compression loading on the top, and the bottom of the shell is under tension. The possibility of extraneous loads in the test cylinders was minimized by employing rollers between moving surfaces and by counterbalancing the conical and end-plate fixtures near their centers of gravity. Rollers were used between the loading frame and the floor supports as well as between the loading frame and the loading jack. Use of the rollers allows axial movement of the cylinder end during application of load and helps to restrict the loads at the

roller locations to normal loads. The rollers were case hardened, as were the surfaces on which they rolled.

The cylinder wall was instrumented on the inside and outside surfaces with strain gages. Displacement transducers along the bottom of the cylinder were used to measure the cylinder deflections. The strain-gage readings, the displacements, and the applied jack load were recorded using a computerized data-acquisition system.

## LOAD INTRODUCTION DETAILS

An examination of strain-gage data from a preliminary test of the cylinder at 30 percent of design load revealed a severe load introduction problem at the ends of the cylinder. A 5.56-cm offset between the centroid radius of the loading ring and the midsurface radius of the shell wall produced an inplane ring rolling moment in the loading rings that produced substantial shell-wall bending at the ends of the shell. The severity of the shell-wall bending caused concern over the possibility of premature buckling of the cylinder.

An analysis of the cylinder was made with BOSOR 4 (ref. 9) using a detailed computer model that included the loading ring, adapter ring, scalloped attachment ring, and corrugated shell wall. (See fig. 5.) Analysis of this model revealed that the scalloped attachment ring rotated with the rolling of the loading ring and caused a large inward displacement of the shell wall near the scalloped attachment rings. Because of low shell-wall hoop stiffness, the inward displacement produced high shell-wall bending strains in addition to the applied axial strain. It was found through computer analysis that the problem could be eliminated by using properly sized spacer blocks with beveled ends (fig. 5) between the adapter rings and the scalloped attachment rings. The aluminum spacer blocks, placed between the adapter rings and the scalloped attachment rings at each bolt holding these rings together (figs. 5 and 6), added 3.81 cm to the overall length of the shell. This brought the total length to 3.19 m including the steel loading rings. As can be seen from figure 7, the spacer blocks served to isolate the rolling of the loading ring from the shell. This significantly reduced the shell-wall bending strains in the cylinder. The axial position along the shell has been normalized with respect to the total shell length $\ell$ of 3.05 m. The strain values have been normalized with respect to the axial strain applied to the corrugation crowns at the top of the cylinder (0° circumferential location as shown in fig. 8), assuming no shell-wall bending. The applied strain is computed from the applied loading intensity and the calculated extensional stiffness given in table 2 for the corrugated shell wall. As can be seen, the shell-wall bending causes the total strain to be nearly twice the applied strain.

A second preliminary test made with the spacer blocks in place indicated that the bending strains in the shell wall were sufficiently reduced to allow a successful buckling test of the cylinder. No buckling or material failures were observed near the loaded ends of the shell during subsequent testing, indicating that the spacer blocks had sufficiently reduced the shell-wall bending strains to prevent a premature failure.

## RESULTS AND DISCUSSION

The experimental axial-strain distribution along the shell length is shown in figure 7, and the axial strains computed by the BOSOR 4 analysis is shown for comparison. These strain values have been normalized with respect to the applied axial strain as described in the preceding section. Although the absolute magnitudes do not compare exactly for experiment and analysis, the reduction trends between strains with and without the spacer blocks compare very favorably.

The applied-strain distribution for a pure applied moment is expected to be a cosine-function distribution around the circumference. The experimental strain distribution is compared in figure 8 with the expected strain distribution and is in close agreement, indicating that near-pure bending was applied.

The vertical displacement along the length of the cylinder relative to its initial position at various load levels during the test are shown in figure 9. The measured displacement at the end of the shell at 100 percent of design load was 0.96 cm.

The location of strain gages on the top section of the cylinder is shown in figure 10, and the response data from these strain gages are shown in figures 11 through 13. Because of bending in the crown, local buckling appears in back-to-back strain-gage data plots as a divergence of the two strain-response curves. At local buckling, one of these two strain-response curves reaches a point of maximum strain before reversing. General instability modes in the shell wall, however, result in a bending moment across the depth of the corrugation. Thus, this mode is characterized by divergence and reversal response curves of the back-to-back strain-gage pairs on adjacent corrugation crowns where one crown is on the inward side of the shell wall and the other crown is on the outward side of the shell wall. As can be seen from the response curves in figures 11 through 13, there is evidence of local and general instability modes occurring simultaneously in the shell wall. The shell walls between rings 1 and 2 and rings 2 and 3 show a pronounced general instability mode behavior. Between rings 3 and 4, however, local buckling behavior occurred prior to general shell instability, as indicated by the responses of gages 33 and 34. The occurrence of this local buckling mode produces a local reduction in crown stiffness, which in turn causes a reduction in overall bending stiffness of the shell wall in that area. As a result, it is probable that a general instability mode developed as a result of the pronounced local instability, resulting in a loss in overall shell-wall bending stiffness in the area. The shell collapsed with a sudden loss of load-carrying capability in a general instability mode between rings 3 and 4 at a load 101 percent of the desired ultimate load. The strain levels produced during this instantaneous collapse were sufficient to cause material separation in the shell wall extending over two-thirds of the circumference of the cylinder. (See fig. 14.)

The measured cylinder mass of 57.08 kg (details in ref. 7) included neither the end rings nor the scalloped attachment rings. As constructed, the 3-m-diameter by 3.05-m-long cylinder yielded a mass per unit area of 1.96 $kg/m^2$.

The measured test load and mass for the graphite-epoxy cylinder are shown on the mass-strength plot of figure 15. The standard mass parameter W/RA is shown on a log-log plot with the standard strength parameter $N_x/R$, where

W mass of shell

A surface area

R radius

$N_x$ wall load per unit width

The open-circle data points in figure 15 were computed from data given in references 10 through 12. The masses of the aluminum shells, not given in these references, were computed for figure 15 using the given nominal geometry values and a 2767-kg/$m^3$ density for aluminum. The mass of rivets or gussets was not included in these calculations. Although the corrugated aluminum shells were not optimized by the same methods used for the graphite-epoxy shell, they do represent a range of low-mass corrugated aluminum construction. By comparison, the corrugated graphite-epoxy cylinder in figure 15 shows a substantial mass-saving potential over the corrugated aluminum shells.

## CONCLUDING REMARKS

Local buckling modes in the shell-wall corrugations were observed to interact with the general shell mode to cause a collapse failure of the shell. Details of the method of load introduction proved to be critical, and a cautious test procedure led to a modification of the load introduction fixtures. This modification prevented a possible premature failure of the test specimen. Comparisons of axial strains along the top of the shell from the test and from a detailed shell-of-revolution analysis were used to prove the concept for modifying the load introduction fixtures. The desired design ultimate load of 157.6 kN/m was reached before buckling, and the overall shell-wall mass was 1.96 kg/$m^2$ for the mass-strength optimized, corrugated, graphite-epoxy cylinder. At 101 percent of the design ultimate load, the shell collapsed suddenly and catastrophically, with severe material separation over two-thirds of the shell circumference. A substantial mass-saving potential was demonstrated compared with available data for corrugated aluminum designs.

Langley Research Center
National Aeronautics and Space Administration
Hampton, VA 23665
June 8, 1982

## REFERENCES


1. Agarwall, Banarsi; and Davis, Randall C.: Minimum-Weight Designs for Hat-Stiffened Composite Panels Under Uniaxial Compression. NASA TN D-7779, 1974.

2. Williams, Jerry G.; and Mikulas, Martin M., Jr.: Analytical and Experimental Study of Structurally Efficient Composite Hat-Stiffened Panels Loaded in Axial Compression. NASA TM X-72813, 1976. (Also available as AIAA Paper No. 75-754.)

3. Anderson, Melvin S.; and Stroud, W. Jefferson: A General Panel Sizing Computer Code and Its Application to Composite Structural Panels. AIAA J., vol. 17, no. 8, Aug. 1979, pp. 892-897.

4. Davis, Randall C.; and Starnes, James H., Jr.: Design Detail Verification Tests for a Lightly Loaded Open-Corrugation Graphite-Epoxy Cylinder. NASA TP-1981, 1982.

5. Johnson, Read, Jr.; Reck, R. J.; and Davis, Randall C.: Design and Fabrication of a Large Graphite-Epoxy Cylindrical Shell. A Collection of Technical Papers - AIAA/ASME 19th Structures, Structural Dynamics and Materials Conference, AIAA, c.1978, pp. 300-310. (Available as AIAA Paper 78-507.)

6. Penton, A. P.; Johnson, R., Jr.; and Freeman, V. L.: Fabrication of Composite Shell Structure for Advanced Space Transportation. Selective Applications of Materials for Products and Energy, Volume 23 of National SAMPE Symposium and Exhibition, Soc. Advance. Mater. & Process Eng., c.1978, pp. 137-149.

7. Johnson, Read, Jr.: Design and Fabrication of a Ring-Stiffened Graphite-Epoxy Corrugated Cylindrical Shell. NASA CR-3026, 1978.

8. Seide, Paul; and Weingarten, V. I.: On the Buckling of Circular Cylindrical Shells Under Pure Bending. Trans. ASME, Ser. E: J. Appl. Mech., vol. 28, no. 1, Mar. 1961, pp. 112-116.

9. Bushnell, David: Stress, Stability, and Vibration of Complex Branched Shells of Revolution: Analysis and User's Manual for BOSOR4. NASA CR-2116, 1972.

10. Peterson, James P.; and Anderson, James Kent: Bending Tests of Large-Diameter Ring-Stiffened Corrugated Cylinders. NASA TN D-3336, 1966.

11. Anderson, James Kent: Bending Tests of Two Large-Diameter Corrugated Cylinders With Eccentric Ring Stiffeners. NASA TN D-3702, 1966.

12. Dickson, John N.; and Brolliar, Richard H.: The General Instability of Ring-Stiffened Corrugated Cylinders Under Axial Compression. NASA TN D-3089, 1966.

TABLE 1.- LAMINA MATERIAL PROPERTIES

| | |
|---|---|
| Lamina thickness, cm | 0.014 |
| Modulus in fiber direction, $GN/m^2$ | 131.0 |
| Modulus in transverse direction, $GN/m^2$ | 13.0 |
| Lamina shear modulus, $GN/m^2$ | 6.41 |
| Major Poisson's ratio | 0.380 |
| Lamina density, $kg/m^3$ | 1522 |

TABLE 2.- MEASURED PROPERTIES OF CORRUGATION WALL

| Wall section | $\frac{\text{Load per unit width}}{\text{Strain}}$, MN/m | | Ratio of transverse to longitudinal strain | |
|---|---|---|---|---|
| | Experimental | Computed | Experimental | Computed |
| Crown $(\pm 45/0_5/\pm 45)$ | 112 | 105 | 0.694 | 0.628 |
| Web $(\pm 45)_S$ | 11.2 | 12.3 | 0.750 | 0.718 |

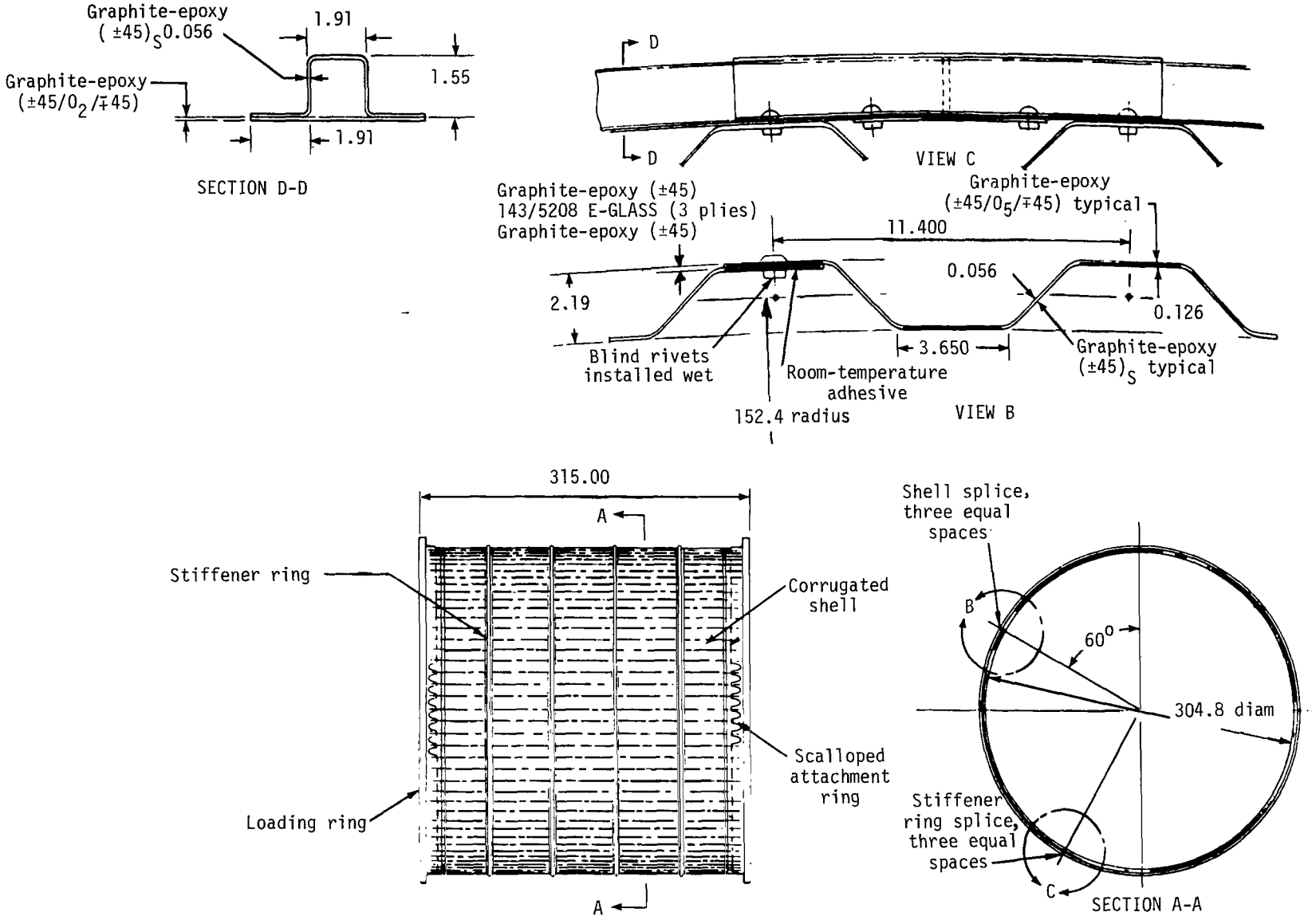


Figure 1.- Configuration of 3-m-diameter graphite-epoxy corrugated cylinder shell. Dimensions are in centimeters.

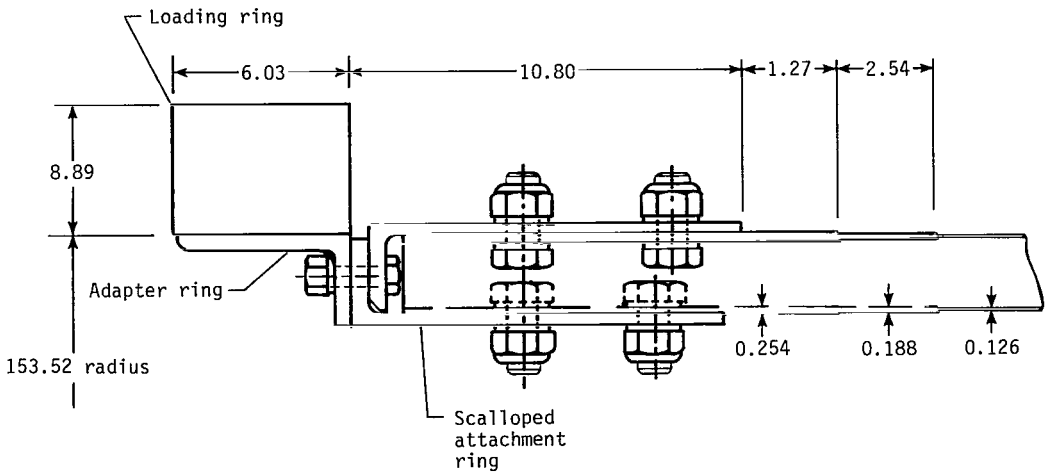


Figure 2.- Loading-ring and scalloped-attachment-ring details at end of cylinder. Dimensions are in centimeters.

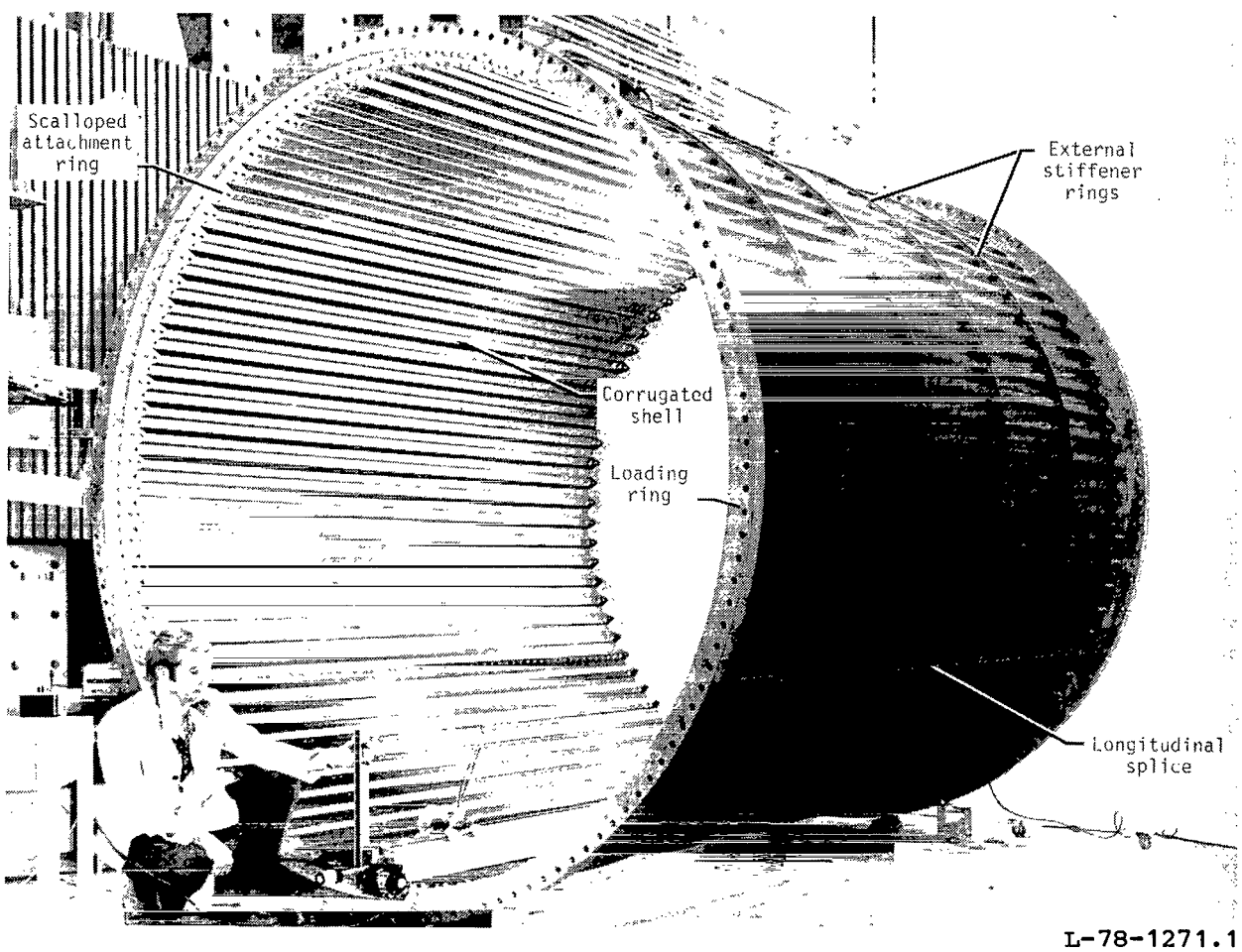


Figure 3.- Photograph of 3-m-diameter corrugated graphite-epoxy cylinder.

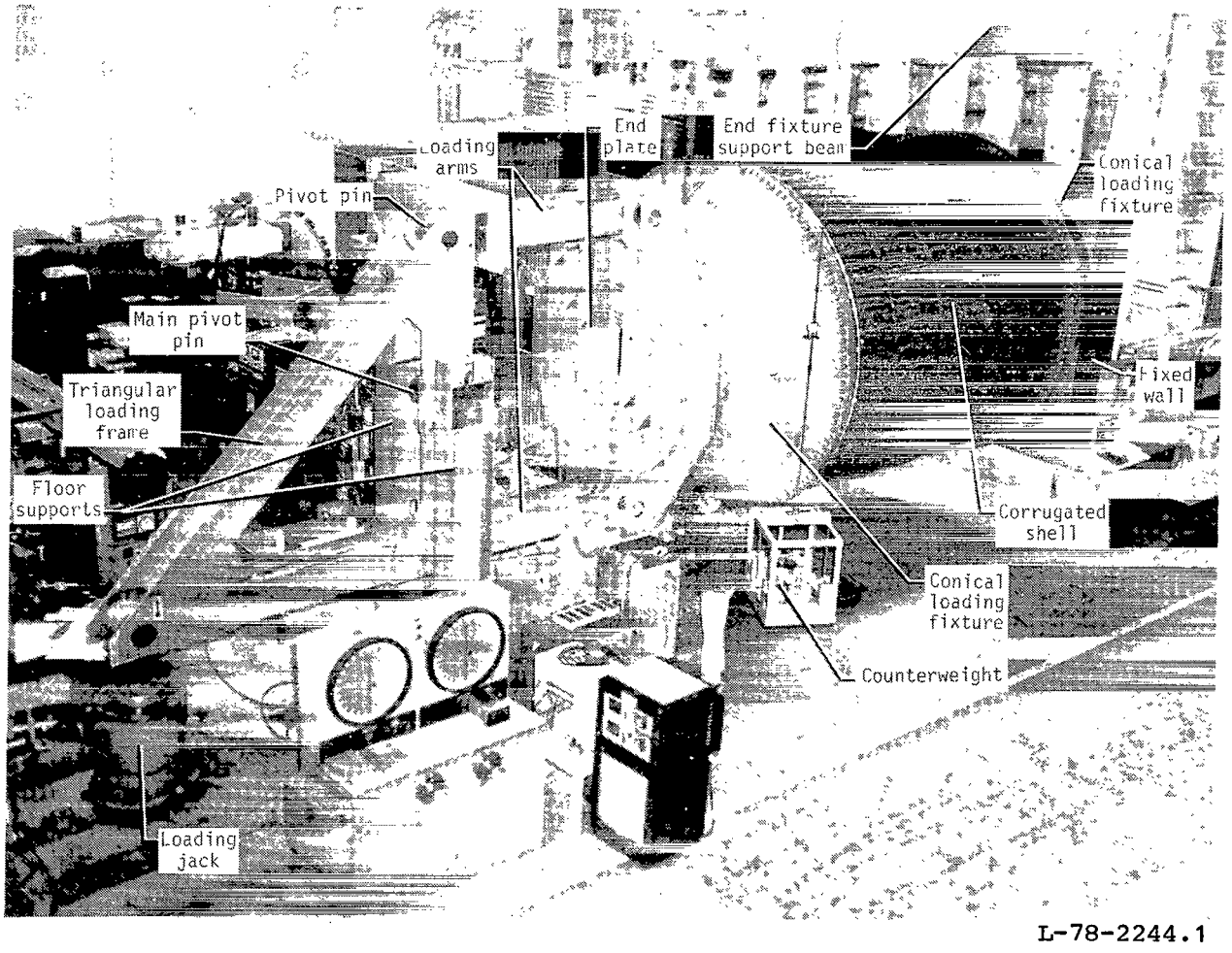


Figure 4.- Test fixture for applying bending moment to corrugated cylinder.

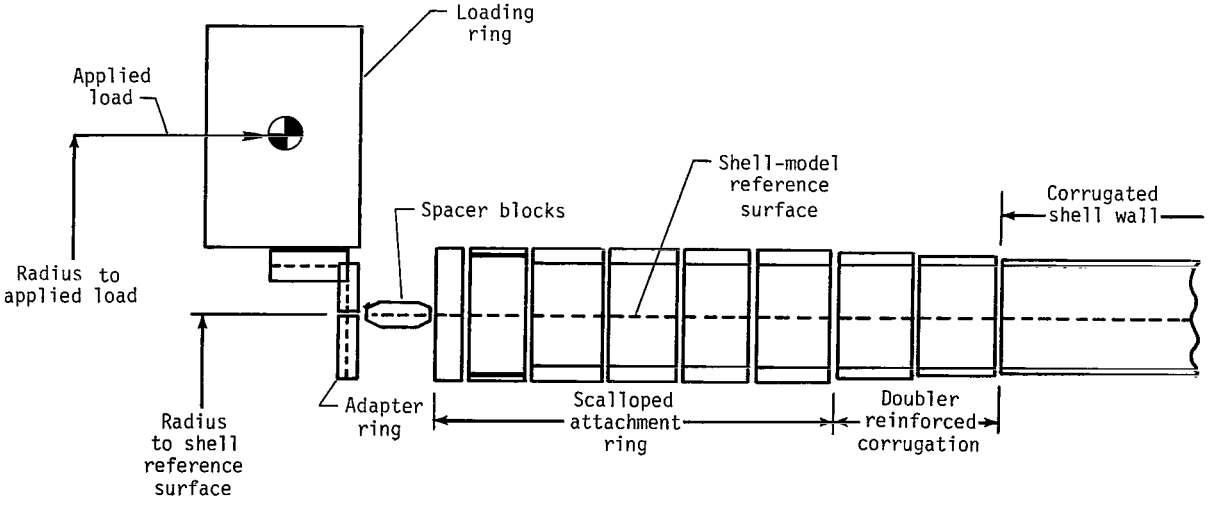


Figure 5.- Schematic of model used in shell analysis.

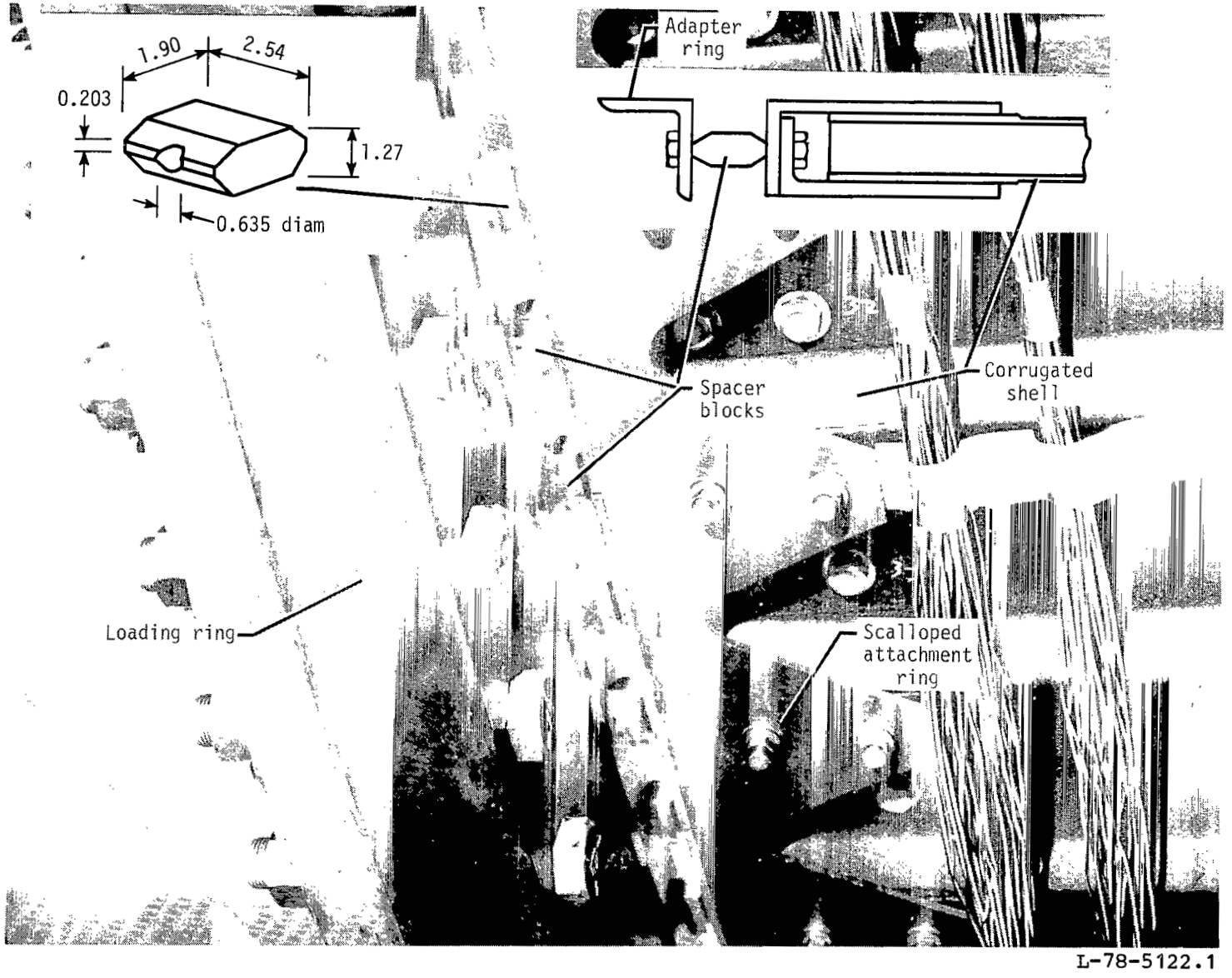


Figure 6.- Spacer blocks in place between scalloped attachment ring and adapter ring. Dimensions are in centimeters.

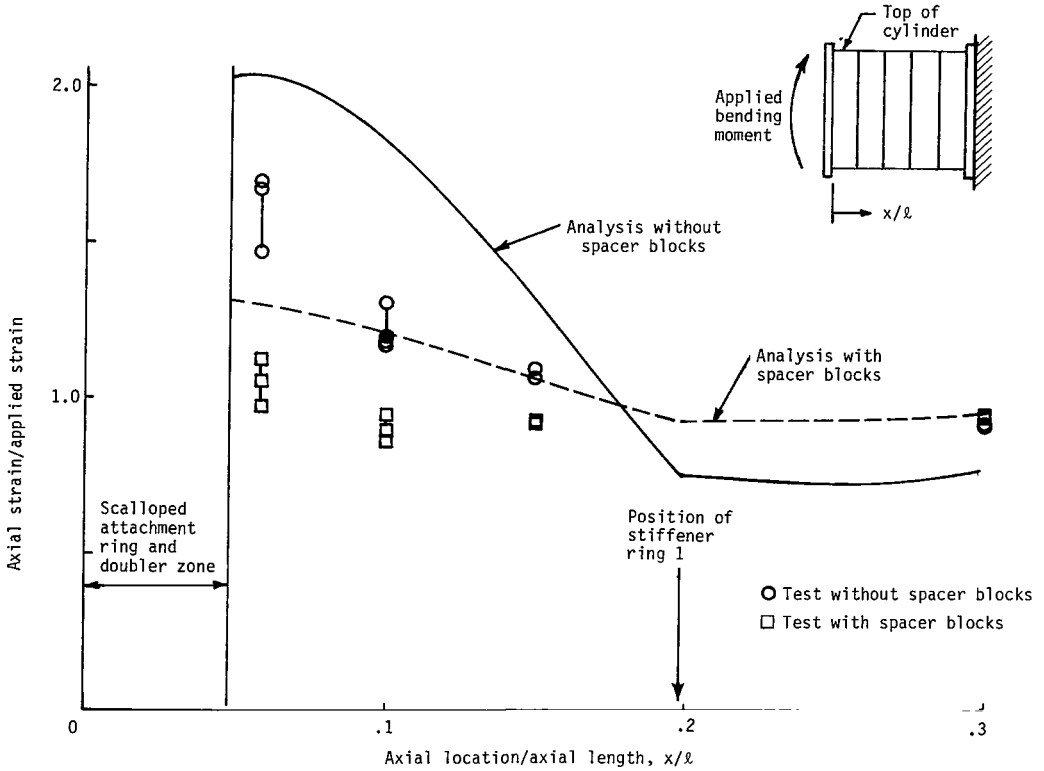


Figure 7.- Axial strain at top of cylinder from analysis and test at 30 percent of design load.

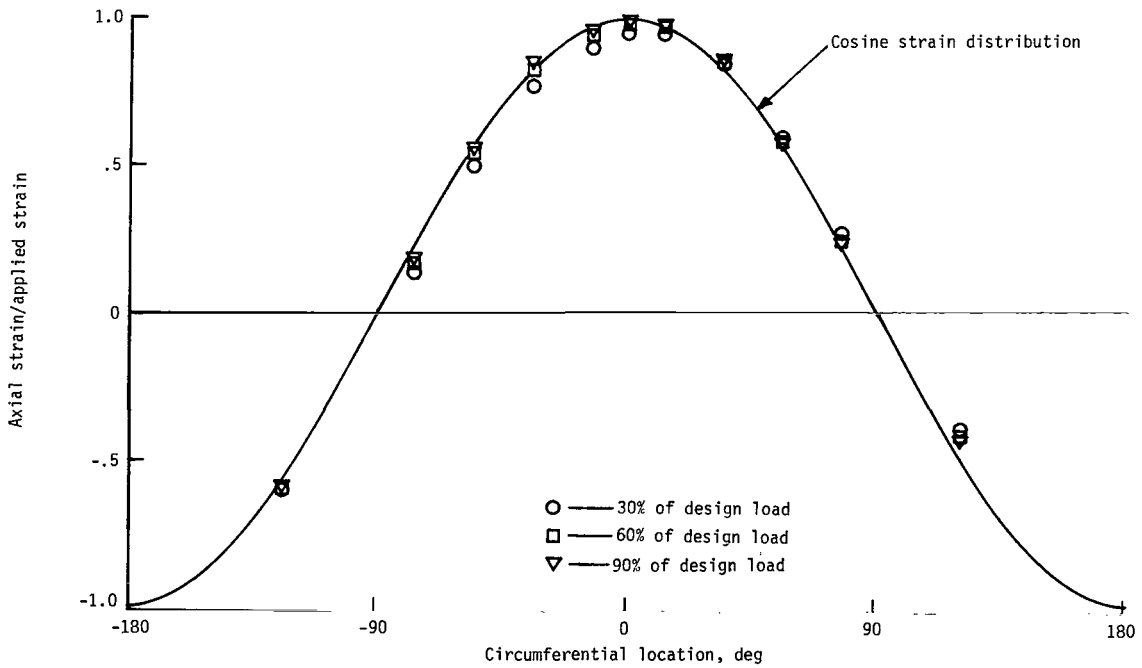


Figure 8.- Axial strain around circumference at midlength of cylinder with spacer blocks in place.

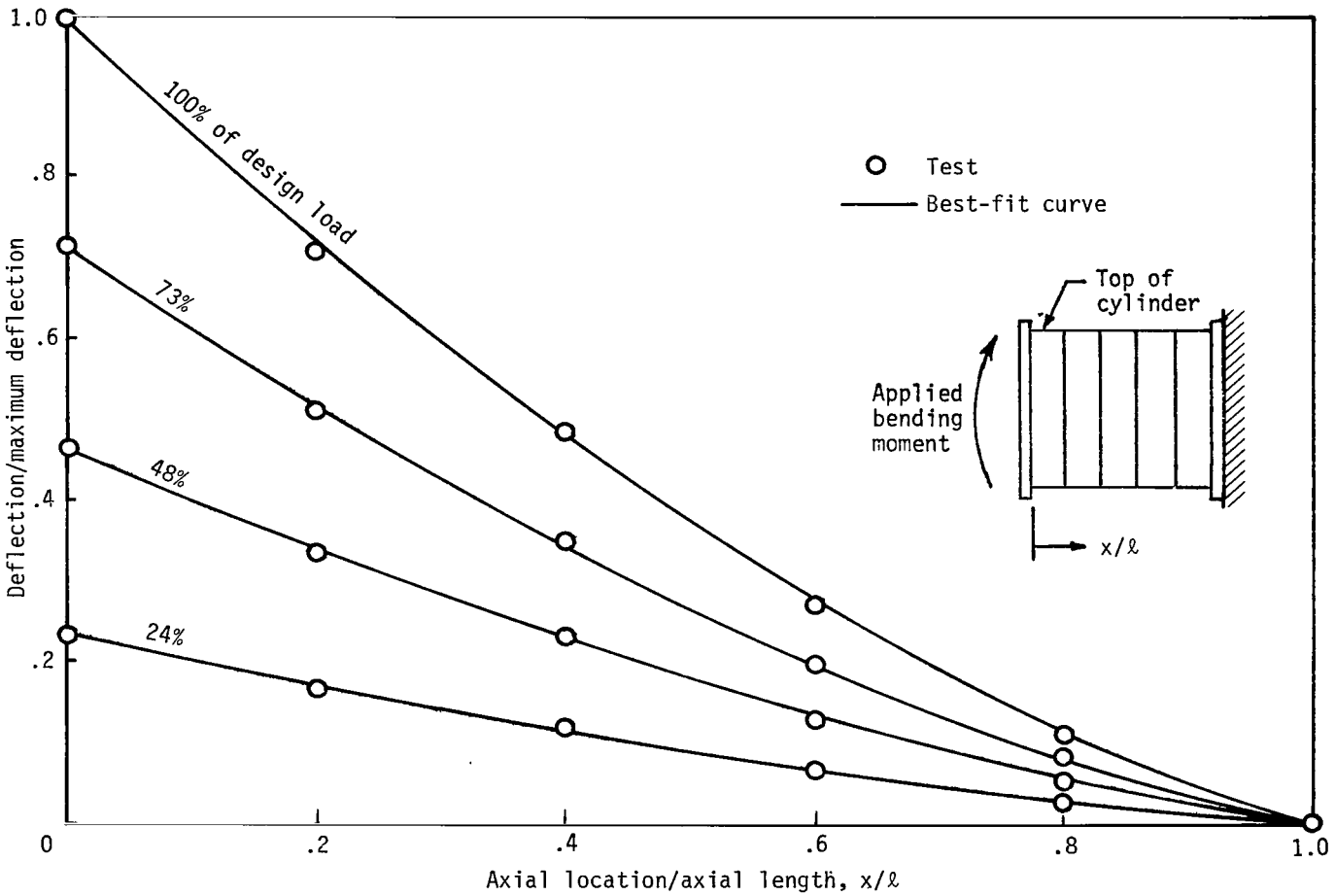


Figure 9.- Deflection of cylinder under bending moment.

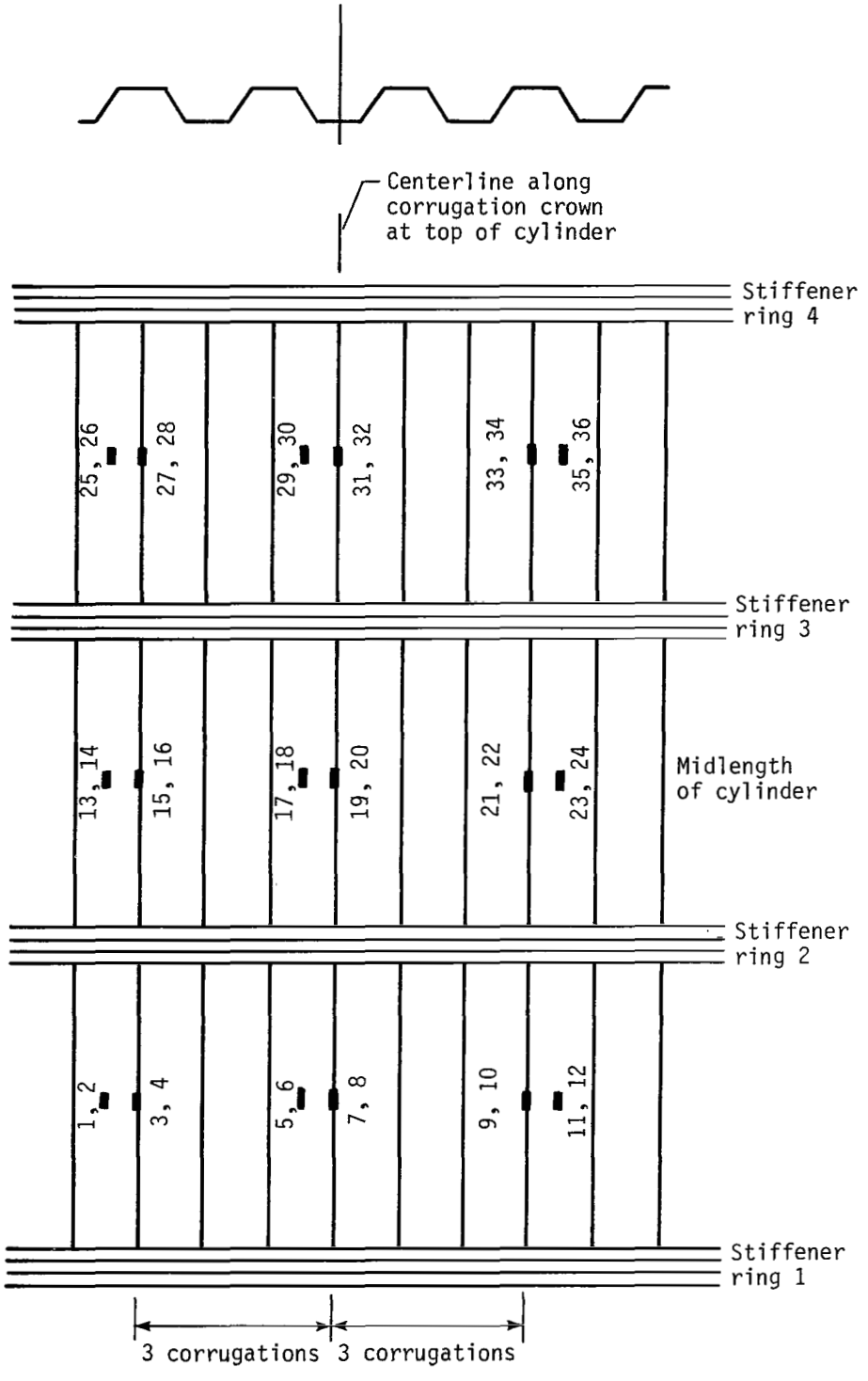


Figure 10.- Strain-gage locations on top of cylinder.

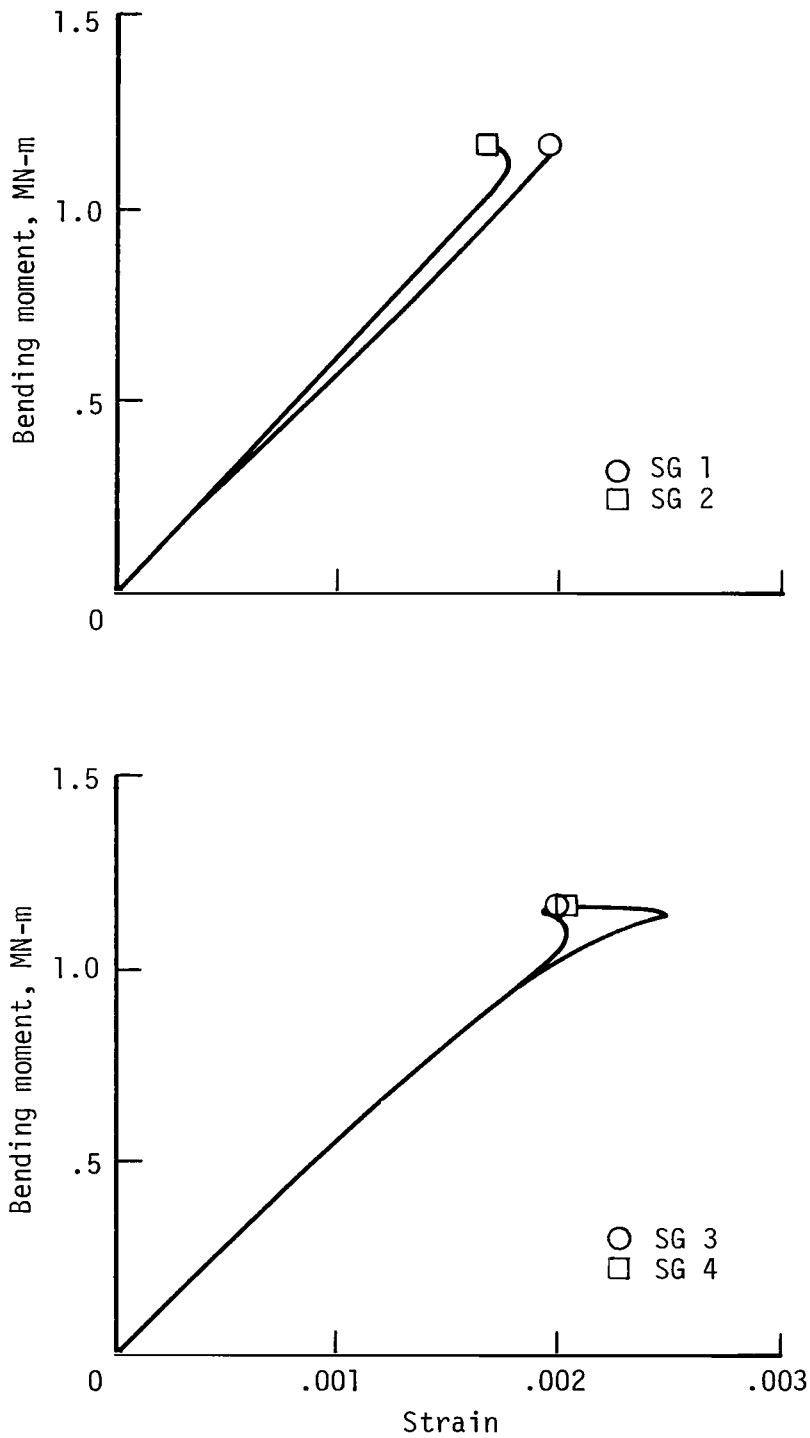


Figure 11.- Strain-gage (SG) responses in section between rings 1 and 2.

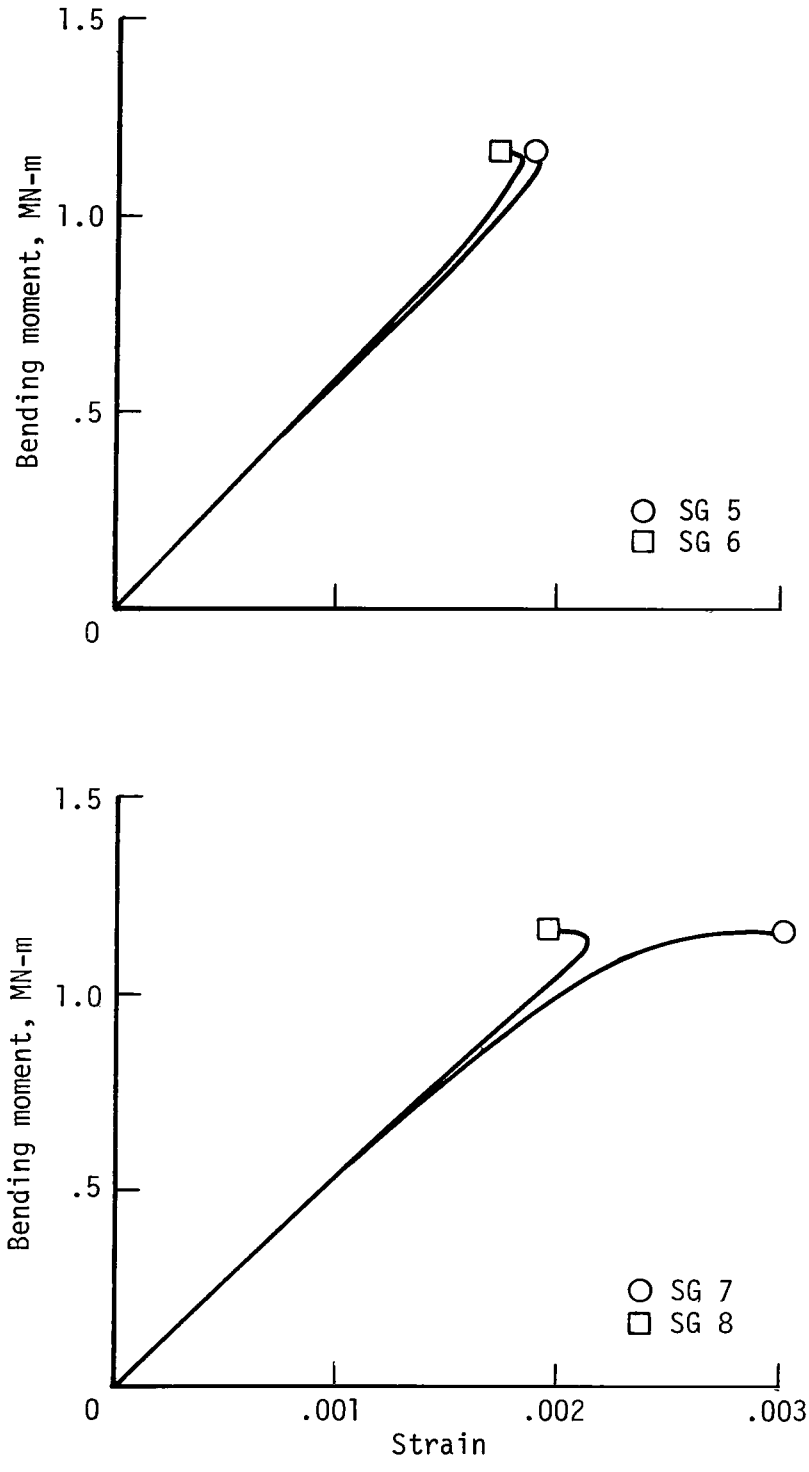


Figure 11.- Continued.

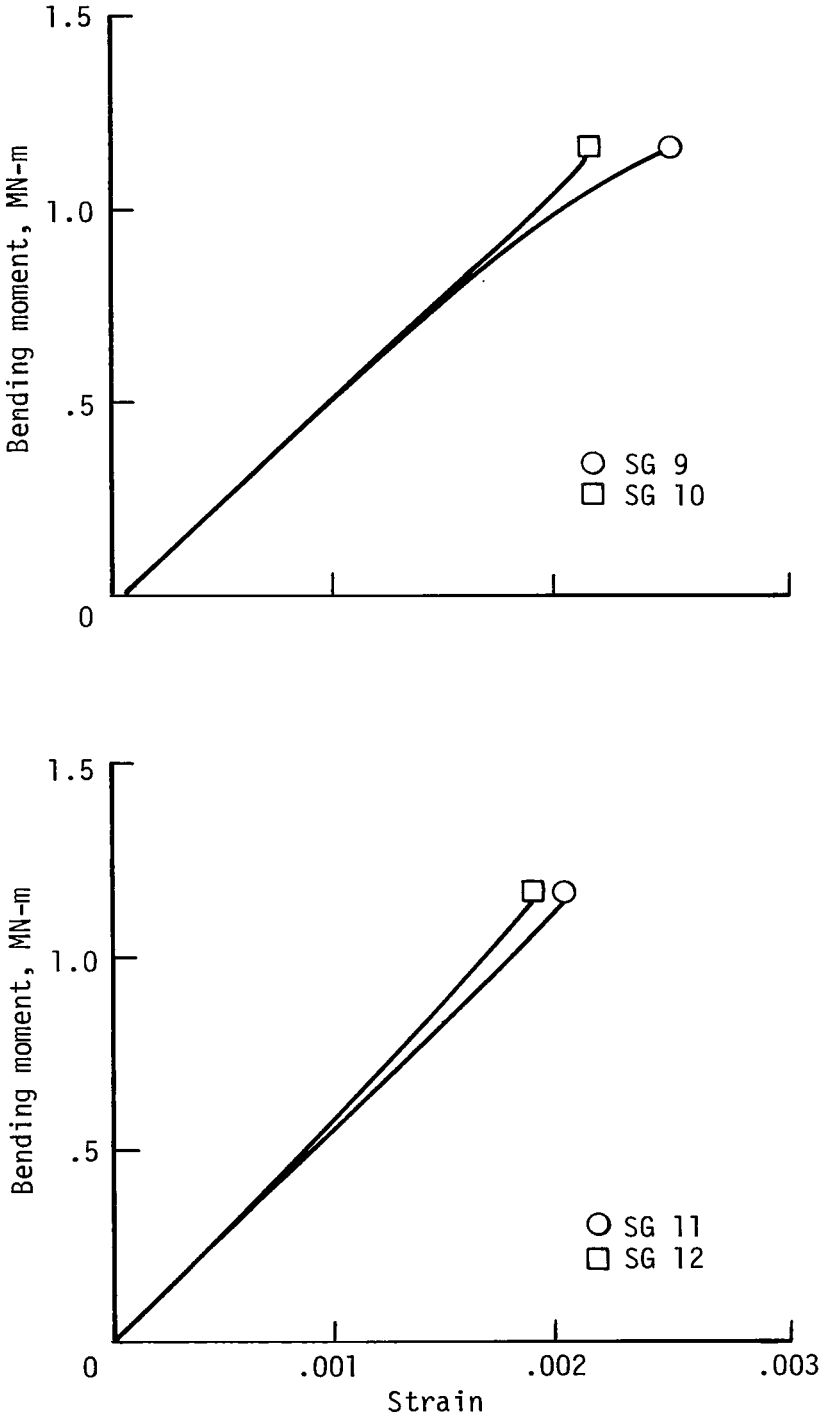


Figure 11.- Concluded.

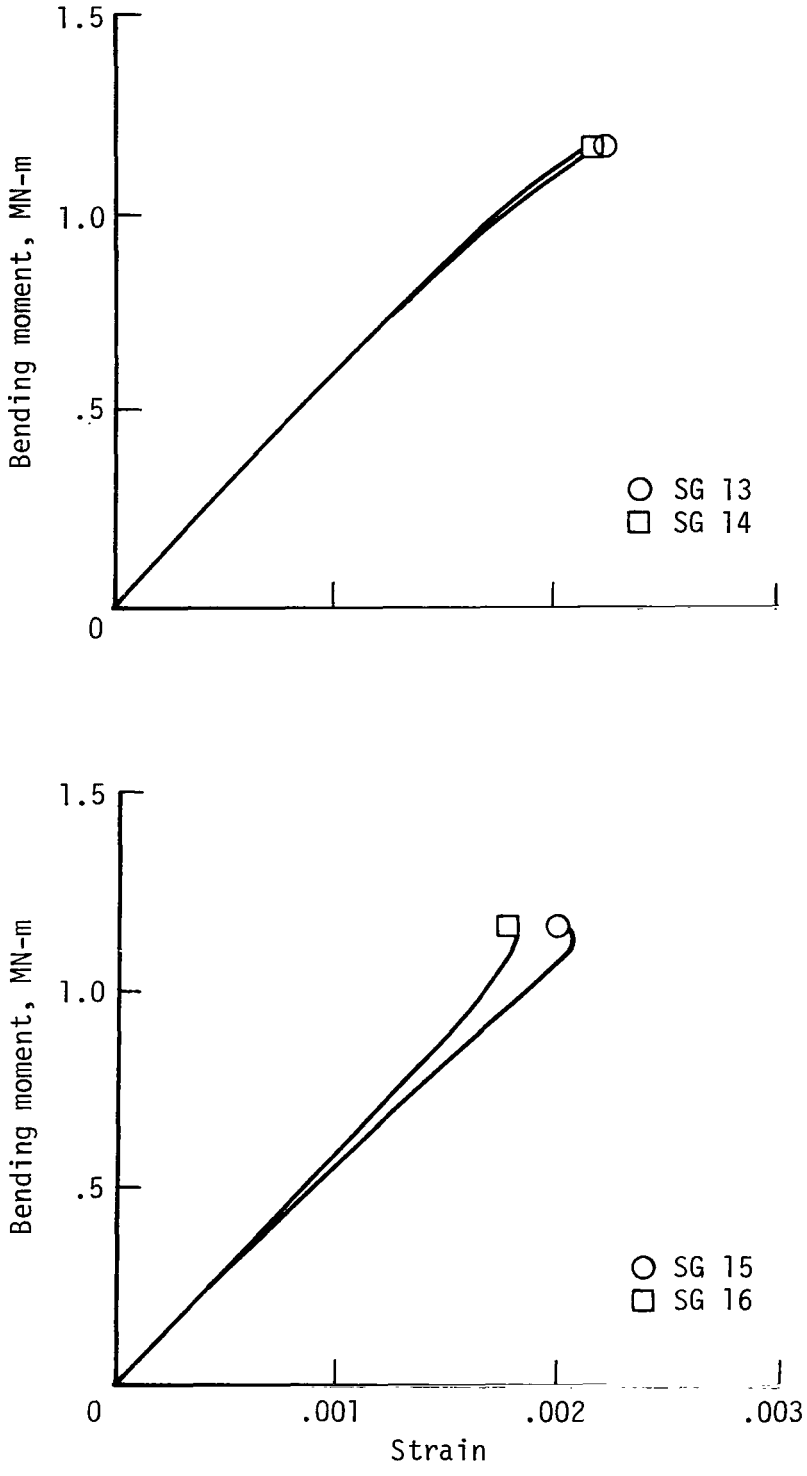


Figure 12.- Strain-gage (SG) responses in section between rings 2 and 3.

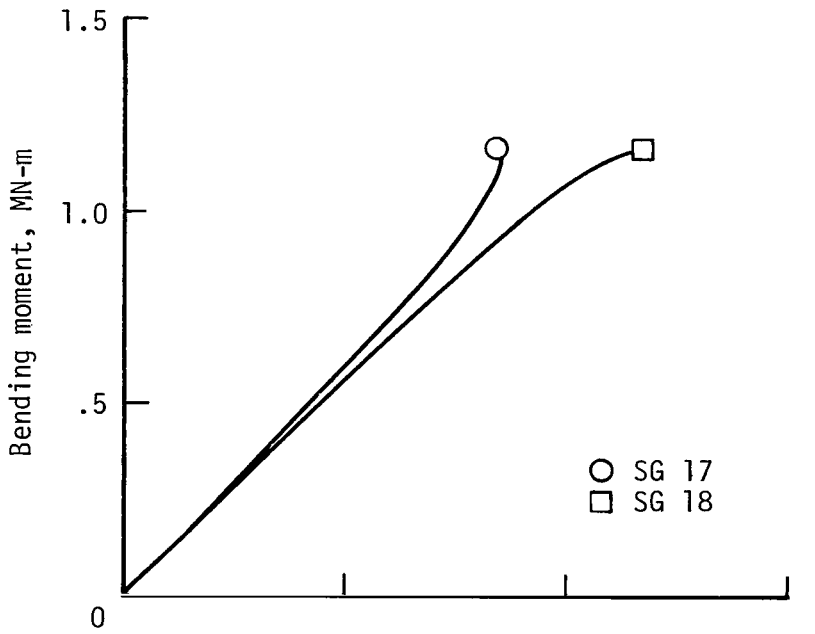


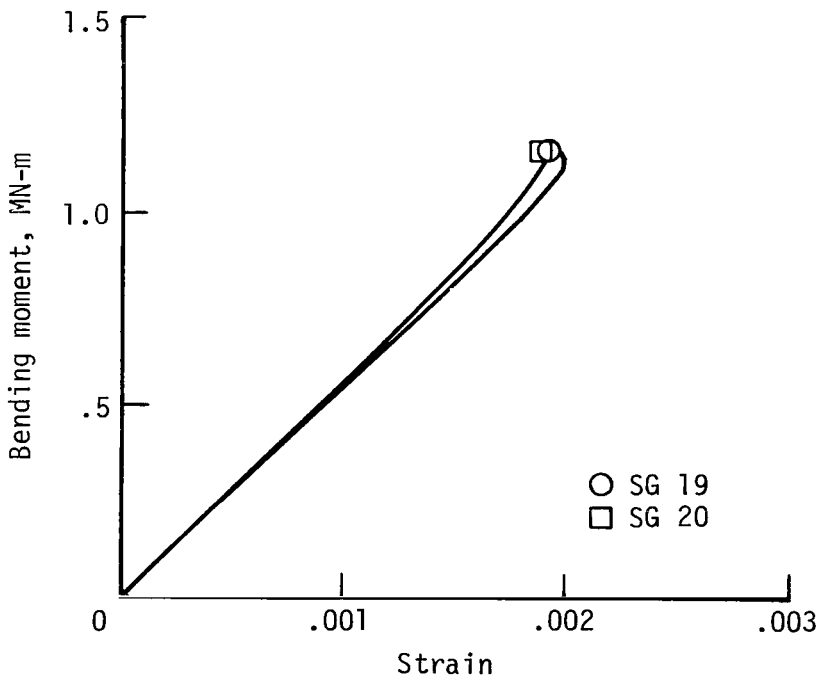


Figure 12.- Continued.

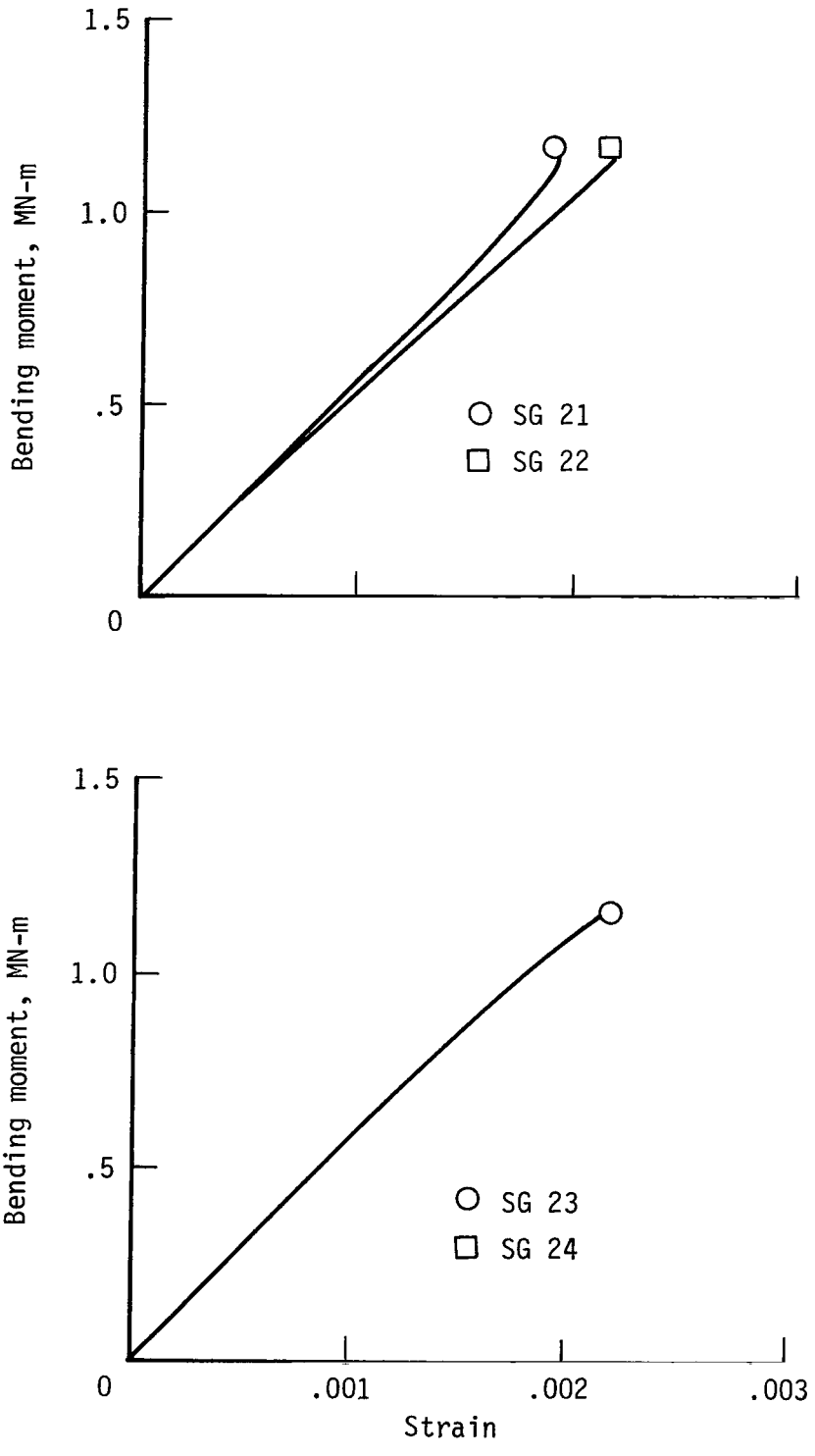


Figure 12.- Concluded.

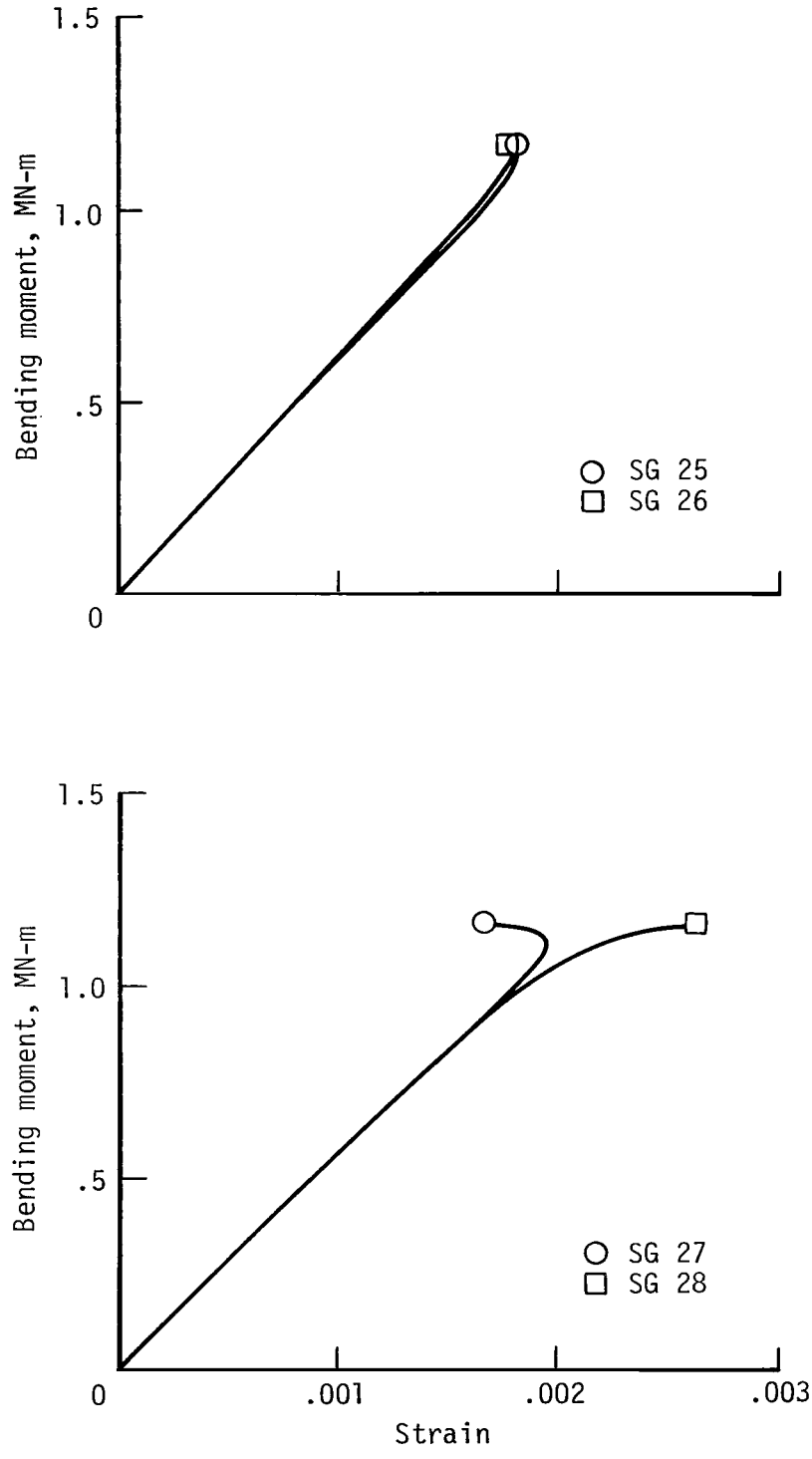


Figure 13.- Strain-gage (SG) responses in section between rings 3 and 4.

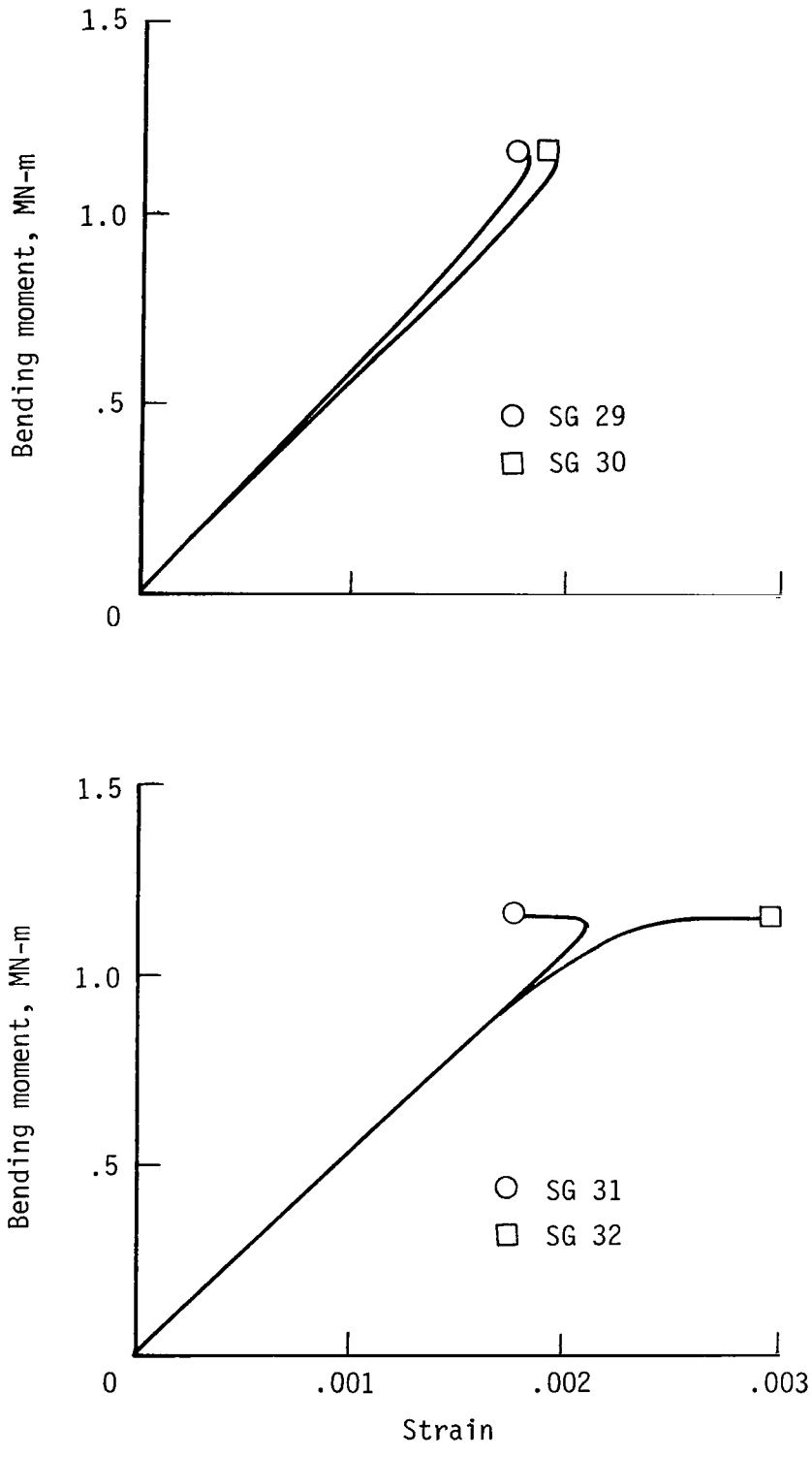


Figure 13.- Continued.

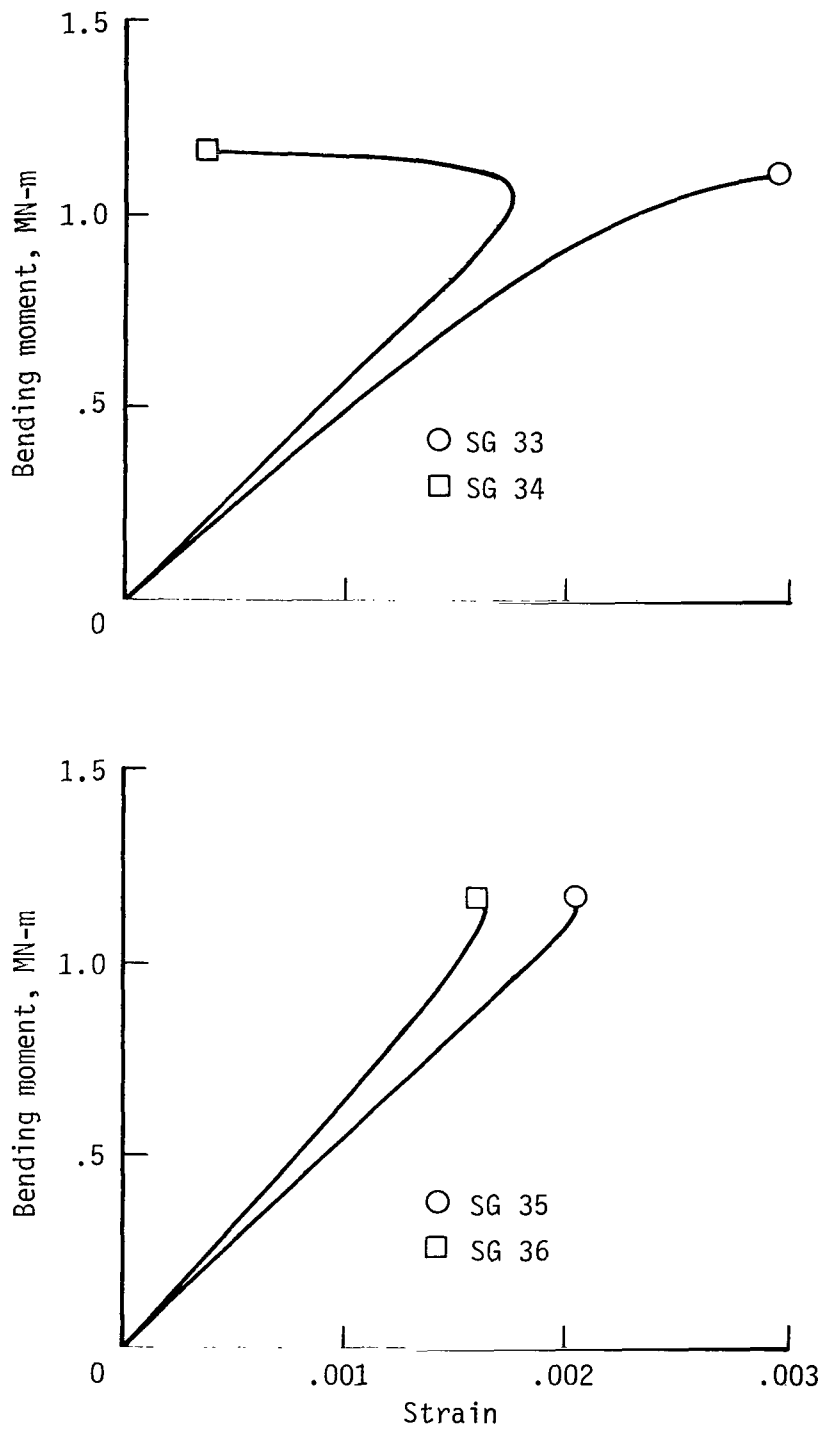


Figure 13.- Concluded.

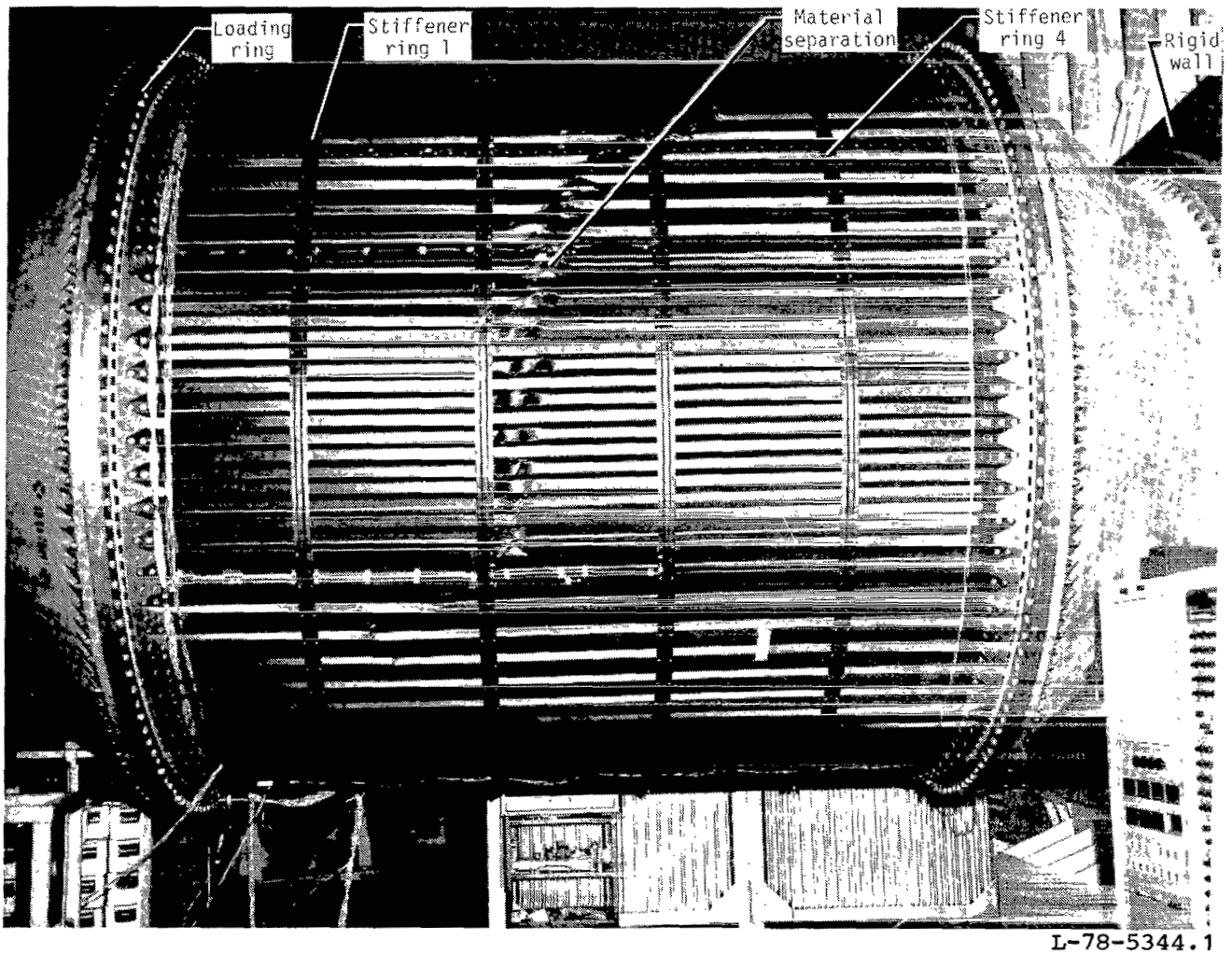


Figure 14.- Photograph of corrugated cylinder immediately after failure with postbuckled load still applied.

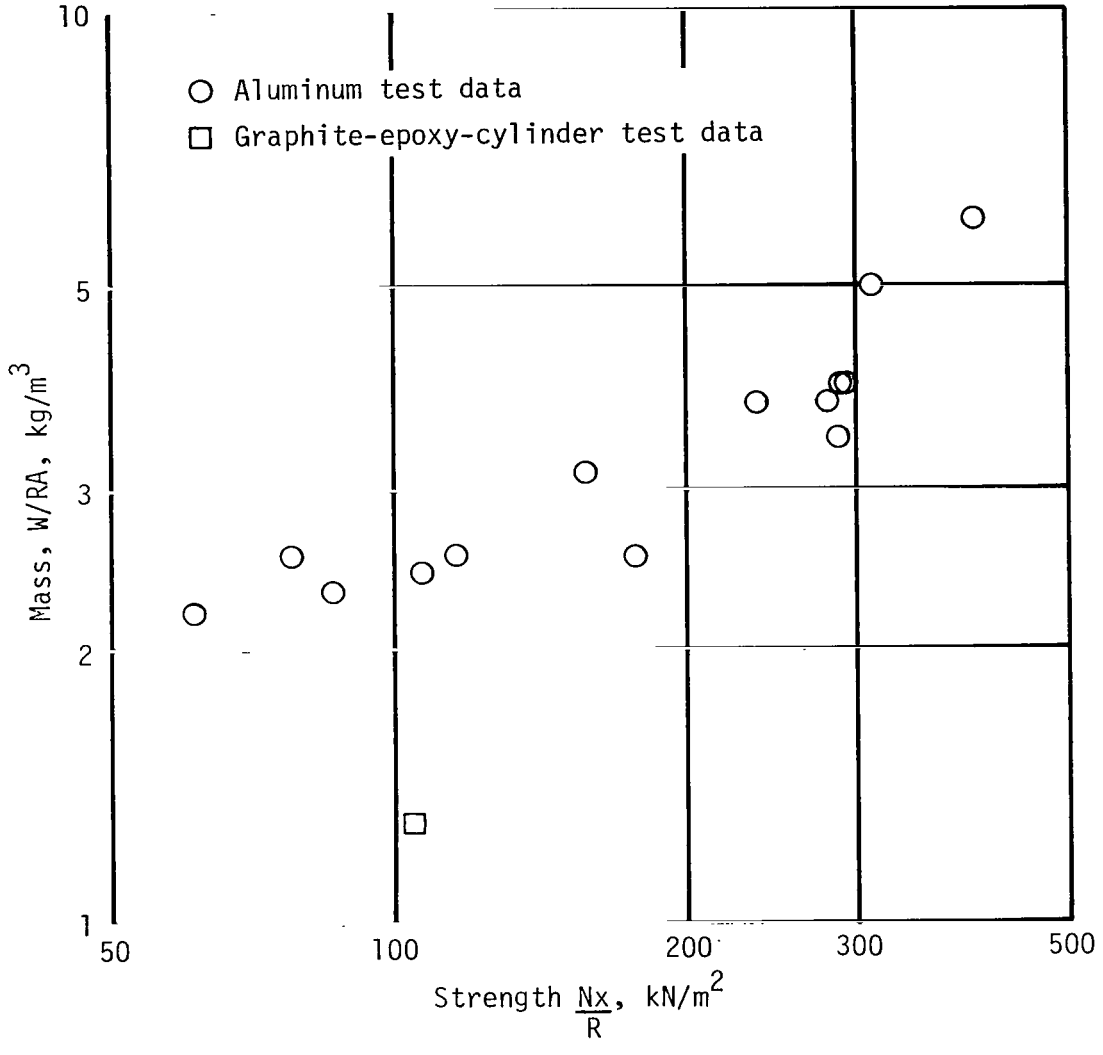


Figure 15.- Mass-strength plot showing mass-saving potential of graphite-epoxy cylinder.

| 1. Report No. | 2. Government Accession No. | 3. Recipient's Catalog No. |
|---|---|---|
| NASA TP-2032 | | |

4. Title and Subtitle
BUCKLING TEST OF A 3-METER-DIAMETER CORRUGATED GRAPHITE-EPOXY RING-STIFFENED CYLINDER

5. Report Date
July 1982

6. Performing Organization Code
506-53-43-02

7. Author(s)
Randall C. Davis

8. Performing Organization Report No.
L-14659

9. Performing Organization Name and Address
NASA Langley Research Center
Hampton, VA 23665

10. Work Unit No.

11. Contract or Grant No.

12. Sponsoring Agency Name and Address
National Aeronautics and Space Administration
Washington, DC 20546

13. Type of Report and Period Covered
Technical Paper

14. Sponsoring Agency Code

15. Supplementary Notes

16. Abstract

A 3-m-diameter by 3-m-long corrugated cylindrical shell with external stiffening rings was tested to failure by buckling. The corrugation geometry for the graphite-epoxy composite cylinder wall was optimized to withstand a compressive load producing an ultimate load intensity of 157.6 kN/m without buckling. The test method used to produce the design-load intensity was to mount the specimen as a cantilevered cylinder and apply a pure bending moment to the end. A load-introduction problem with the specimen was solved by using the BOSOR 4 shell-of-revolution computer code to analyze the shell and attached loading fixtures. The cylinder test loading achieved was 101 percent of design ultimate, and the resulting mass per unit of shell-wall area was 1.96 $kg/m^2$.

| 17. Key Words (Suggested by Author(s)) | | 18. Distribution Statement |
|---|---|---|
| Test | Axial compression | Unclassified - Unlimited |
| Buckling | Bending | |
| Corrugated shell | Optimized design | |
| Graphite-epoxy | | |
| Composite | | Subject Category 39 |

| 19. Security Classif. (of this report) | 20. Security Classif. (of this page) | 21. No. of Pages | 22. Price |
|---|---|---|---|
| Unclassified | Unclassified | 27 | A03 |

For sale by the National Technical Information Service, Springfield, Virginia 22161

NASA-Langley, 1982

1 1 1U,D, 820702 S00903DS
DEPT OF THE AIR FORCE
AF WEAPONS LABORATORY
ATTN: TECHNICAL LIBRARY (SUL)
KIRTLAND AFB NM 87117